

factory performance for computing the scattering amplitudes; (ii) the equations for shape parameters decouple and the numerical procedure for the inversion problem becomes very efficient, thus resulting in a very satisfactory shape recovery for exact data. Due to the ill-posed nature of the inverse problems, shape recovery and its resolution were found to be sensitive to the data noise. However, shape recovery of the part of the scatterer facing the line source was found to be more satisfactory. Thus, changing the location of the line source can be used in a stabilization procedure to reduce the effect of noise on the inversion result.

ACKNOWLEDGMENTS

We wish to thank Dr. Rainer Kress for helpful communication regarding the combined double- and single-layer approach for the Helmholtz equation.

REFERENCES

1. J.A. Kong, *Electromagnetic wave theory*, Wiley, New York, 1986.
2. C. Eftimiu, *Electromagnetic scattering by rough conducting circular cylinders I: Angular corrugation*, *IEEE Trans Antennas Propagat* 36 (1988), 659–663.
3. D. Colton and R. Kress, *Inverse acoustic and electromagnetic scattering theory*, Springer Verlag, New York, 1992.
4. R. Kress, *On the numerical solution of a hypersingular integral equation in scattering theory*, *J Comp Appl Math* 61 (1995), 345–360.
5. A.E. El-Rouby, F.T. Ulaby, and A.Y. Nashahibi, *MMW scattering by rough lossy dielectric cylinders and tree trunks*, *IEEE Trans Geosci Remote Sensing* 40 (2002), 871–879.
6. N.C. Skaropoulos and D.P. Chrissoulidis, *On the accuracy of perturbative solutions to wave scattering from rough closed surfaces*, *J Acoust Soc Am* 114 (2003), 726–736.
7. G. Meyer, *The method of lines for Poisson's equation with nonlinear or free boundary conditions*, *Numer Math* 29 (1978), 329–344.
8. J.G. Ma, T.K. Chia, T.W. Tan, and K.Y. See, *Electromagnetic wave scattering from 2-D cylinder by using the method of lines*, *Microwave Opt Technol Lett* 24 (2000), 275–277.
9. M.A. Hooshyar, *An inverse problem of electromagnetic scattering and the method of lines*, *Microwave Opt Technol Lett* 29 (2001), 420–426.
10. D. Zwillinger, *Handbook of differential equations*, Academic Press, New York, 1989.
11. E. Isaacson and H.B. Keller, *Analysis of Numerical Methods*, Wiley, New York, 1966.
12. N. Bleistein, *Mathematical methods for wave phenomena*, Academic Press, New York, 1984.
13. G.F. Forsythe, M.A. Malcolm, and C.B. Moler, *Computer Methods for Mathematical Computations*, Prentice Hall, New York, 1976.

© 2004 Wiley Periodicals, Inc.000;:201

EFFECT OF LOSSES AND DISPERSION ON THE FOCUSING PROPERTIES OF LEFT-HANDED MEDIA

R. Marqués and J. Baena

Dept. de Electrónica y Electromagnetismo
Universidad de Sevilla
41012 Sevilla, Spain

Received 15 October 2003

ABSTRACT: *By means of an analysis of the field radiated by a point source placed in front of an infinite left-handed slab, the effect of losses and dispersion on the focusing properties of continuous left-handed media are analyzed. It is shown that subwavelength focusing of point-like quasi-monochromatic sources can be achieved by using physical left-*

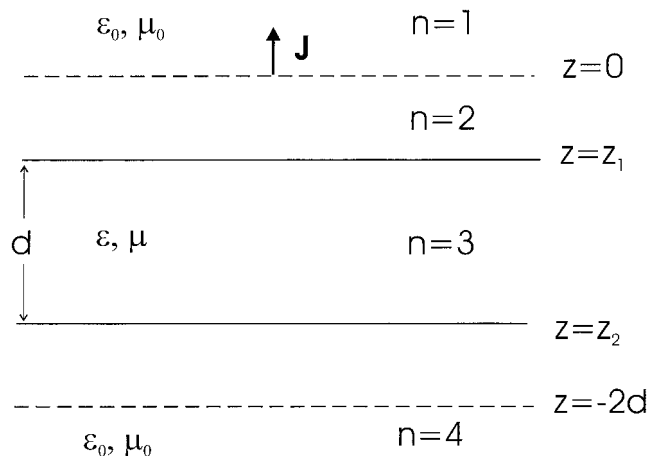


Figure 1 The structure under analysis: a point source over an isotropic slab of permittivity ϵ , permeability μ , and width d . The focus plane at $z = -2d$ when $\epsilon = -\epsilon_0$ and $\mu = -\mu_0$ is also shown

handed slabs, provided some conditions are fulfilled. These conditions are qualitative and quantitatively analyzed. Numerical examples that show the accuracy of this analysis are provided. Finally, the proposed electromagnetic analysis and the geometrical Veselago's demonstration of over-wavelength focusing by left-handed slabs are found to be mutually consistent. © 2004 Wiley Periodicals, Inc. *Microwave Opt Technol Lett* 41: 290–294, 2004; Published online in Wiley InterScience (www.interscience.wiley.com). DOI 10.1002/mop.20119

Key words: *left-handed media; negative refractive index; perfect lens*

1. INTRODUCTION

In 1987, Veselago [1] predicted that hypothetical left-handed media (LHM) (media with dielectric permittivity ϵ and magnetic permeability μ that are both negative) would exhibit negative refractive index, and that this fact should produce the focusing of a point-like source by a LHM slab. After the practical realization of these media, reported by Smith et al. [2] and in subsequent works [3–5], considerable attention has been paid to those topics [6–10]. In addition to Veselago's predictions [1], it has been predicted [6] that a LHM slab having $\mu = -\mu_0$ and $\epsilon = -\epsilon_0$ (where ϵ_0 and μ_0 are the dielectric permittivity and magnetic permeability of a vacuum, respectively) should produce subwavelength perfect focusing of electromagnetic sources. However, all these predictions have not gone unchallenged and it has been claimed that both losses and dispersion will destroy these effects [8–10]. Therefore, further research, both theoretical and experimental, is needed. In this work, the problem of the sub- and/or over-wavelength focusing of a realistic point-like source by an infinite LHM slab is addressed theoretically. Our aim is to find the physical limitations of this phenomenon, arising from the unavoidable presence of dispersion and losses in such media.

The paper is organized as follows. First, the electromagnetic field radiated from a monochromatic point source

$$\mathbf{J} = I_0 \hat{\mathbf{z}} \delta(x) \delta(y) \delta(z) \exp\{j\omega t\} \quad (1)$$

through an infinite slab of permittivity ϵ , permeability μ , and thickness d (see Fig. 1) is analyzed. In order to simplify the analysis, the current source is directed along the axis perpendicular to the slab. However, a very similar analysis holds for more general point sources [11]. The analysis leads to a closed and analytical expression for the transfer function, given by Eq. (6). It

is important to have an analytical expression for this function, since numerical analysis (which implies a discretization of the space and time) may lead to spurious limitations on the focusing properties of continuous media [12].

Once the radiated fields have been computed for arbitrary ε and μ , these parameters are equated to $-\varepsilon_0$ and $-\mu_0$, respectively, and the focusing of the point source at a distance $2d$ of the source is analyzed. Next, material losses are taken into account. It is shown that the focusing of a monochromatic point-like source is mainly limited by the slab thickness and material losses, rather than by the free-space wavelength. Then, the effect of dispersion for a point-like source operating for a finite time interval, Δt , is considered. After this analysis, the limits of over- and sub-wavelength focusing in dispersive LHM slabs are discussed.

2. ANALYSIS

Figure 1 shows the configuration under analysis. In this configuration the magnetic-field component H_z vanishes and the electromagnetic field is deduced from a scalar potential ϕ as follows [11]:

$$\mathbf{E} = \nabla_t \frac{\partial \phi}{\partial z} - \hat{\mathbf{z}} \nabla_t^2 \phi, \quad (2)$$

$$\mathbf{H} = -j\omega\varepsilon\hat{\mathbf{z}} \times \nabla_t \phi, \quad (3)$$

where ∇_t is the transverse differential operator $\nabla_t = \hat{\mathbf{x}}\partial_x + \hat{\mathbf{y}}\partial_y$. The potential ϕ must satisfy the Helmholtz wave equation in each subregion of Figure 1, with the appropriate boundary conditions at $z = 0, z_1, z_2$. In the spectral domain, where the transform, \tilde{F} , of a physical variable, F , is defined as:

$$\tilde{F}(k_x, k_y, z, t) = \iint dx dy F(x, y, z, t) e^{-j(k_x x + k_y y)}, \quad (4)$$

the scalar potential in each subregion n of Figure 1 is given by

$$\tilde{\phi} = A_n(k_x, k_y) e^{-j\beta_n z} + B_n(k_x, k_y) e^{j\beta_n z}, \quad (5)$$

where $\beta_n = \sqrt{\omega^2 \varepsilon_n \mu_n - k_x^2 - k_y^2}$. For physical fields, we must have $B_1 = A_4 = 0$. The remaining coefficients are determined from the boundary conditions at the interfaces at $z = z_1, z_2$, and at the source plane, $z = 0$ [11]. After solving for A_n, B_n , the spectral domain potential $\tilde{\phi}$ for $z \leq z_2$ is found to be:

$$\tilde{\phi} = \frac{2\beta\varepsilon I_0 \exp\{j\beta_0(z+d)\}}{\omega\{(\beta\varepsilon_0 - \beta_0\varepsilon)^2 \exp\{-j\beta d\} - (\beta\varepsilon_0 + \beta_0\varepsilon)^2 \exp\{j\beta d\}\}}, \quad (6)$$

where β and β_0 are given by $\beta = \sqrt{\omega^2 \varepsilon \mu - k_x^2 - k_y^2}$ and $\beta_0 = \sqrt{\omega^2 \varepsilon_0 \mu_0 - k_x^2 - k_y^2}$. Note that this analysis does not depend on the choice of the sign for the square root in the definition of β , since Eq. (6) does not change after the change $\beta \rightarrow -\beta$. Thus, Eq. (6) is independent of any hypothesis about the correct choice of this sign in an infinite LHM. Moreover, since the coefficients in Eq. (5) are uniquely determined by the boundary conditions at $z = 0, z_1, z_2$ and by the Sommerfeld radiation condition at $z = \pm\infty$, the solution given by Eq. (6) is unique.

3. EFFECT OF LOSSES

If, for a given frequency ω_0 , the constitutive parameters of the slab become $\varepsilon(\omega_0) = -\varepsilon_0$ and $\mu(\omega_0) = -\mu_0$, then $\beta = \beta_0$ and the above analysis shows that $A_2 = B_3 = 0$ in Eq. (5), and Eq. (6) reduces to

$$\tilde{\phi}_0(\omega_0) = -\frac{I_0}{2\omega_0\beta_0(\omega_0)\varepsilon_0} \exp\{j[\beta_0(\omega_0)(z+2d)]\}, \quad (7)$$

and

$$\tilde{\phi}(z = -2d; \omega_0) = -\frac{I_0}{2\omega_0\beta_0(\omega_0)\varepsilon_0} = \tilde{\phi}(z = 0; \omega_0), \quad (8)$$

for all k_x and k_y . Since the reflection coefficient vanishes and the spectral components of the scalar potential at the source plane ($z = 0$) are exactly reproduced at the focus plane ($z = -2d$) for any values of the spectral variables, the electromagnetic field will be also exactly reproduced at this plane [6]. However, from Eq. (7) it is easily realized that, for $z_2 > z > -2d$, the spectral components of $\tilde{\phi}(k_x, k_y, z; \omega_0)$ diverge when $k_x, k_y \rightarrow \pm\infty$ (and the same happens for $-2z_1 > z > z_2$, although it is not explicitly shown here). This fact is a serious objection to this theory and the main argument in the refutation reported by Garcia et al. [8]. Nevertheless, the aforementioned uniqueness of (6) clearly precludes any attempt of obtaining any other physical solution for $\tilde{\phi}(k_x, k_y, z; \omega_0)$, thus leading to a paradox. This paradox is solved by considering that all physical LHM must incorporate some amount of material losses (as was, in fact, noted in [8]). Thus, at $\omega = \omega_0$ we have $\varepsilon(\omega_0) = -\varepsilon_0 - j\varepsilon''(\omega_0)$ and $\mu = -\mu_0 - j\mu''(\omega_0)$. Therefore, the quantity $(\beta\varepsilon_0 + \beta_0\varepsilon)^2$ in the denominator of Eq. (6) do not vanish exactly at $\omega = \omega_0$. Thus, for large enough k_x and/or k_y , the second summand in the denominator of Eq. (6) will dominate over the first summand, and the aforementioned divergence of $\tilde{\phi}$ for $k_x, k_y \rightarrow \pm\infty$ is avoided. In fact, for $k_t = \sqrt{k_x^2 + k_y^2} \rightarrow \infty$ and $\varepsilon'' \neq 0$, after taking the appropriate limits, we obtain

$$|\tilde{\phi}| \sim \exp\{k_t z\}, \quad (9)$$

which goes to zero for all negative values of z and, in particular, in the entire domain of the application of Eq. (6), that is, for $z < z_2$. However, for small values of k_t (we will precisely describe this condition in the following), $\tilde{\phi}(z = -2d)$ can be still approximated by Eq. (7) and, therefore, the corresponding spectral components are still amplified through the LHM slab and reproduced at the image plane. Therefore, although strictly focusing is not possible (speaking perfect), subwavelength focusing is possible in physical LHM slabs, and perfect focusing appears as a physical limit achieved when losses tends to zero.

As explained previously, a given spectral-domain field component will be reproduced at the focus if, for this particular component, the first summand in the denominator of Eq. (6) dominates over the second one. For large values of k_x and/or k_y , we can take $\beta(\omega_0) \sim \beta_0(\omega_0) \sim -j\sqrt{k_x^2 + k_y^2}$ in the denominator of Eq. (6). Thus, the aforementioned condition for the validity of Eqs. (7) and (8) can be expressed as

$$k_t d < \ln\left(2 \frac{\varepsilon_0}{\varepsilon''}\right), \quad (10)$$

where k_t is the transverse spectral wavenumber $k_t = \sqrt{k_x^2 + k_y^2}$. Eq. (10) shows that the subwavelength focusing properties of an LHM slab are mainly limited by the thickness and losses of the slab, and that the maximum value of $k_t, k_{t,max}$, for which the corresponding spectral component reproduced at the image plane has a logarithmic dependence on the loss tangent, $\tan \delta = \varepsilon''/|\varepsilon'|$. This fact is illustrated in Figure 2. In this figure, the deviation factor from the ideal behavior of $\tilde{\phi}$,

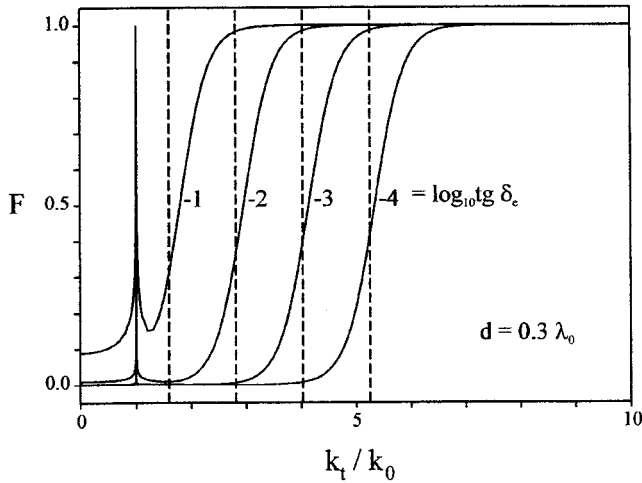


Figure 2 The deviation factor from the ideal behavior F as a function of k_t/k_0 for a LHM slab with thickness $d = 0.3\lambda_0$ and for different values of the dielectric loss tangent. The values of $k_{t,max}/k_0$ obtained from Eq. (10) are also shown (dashed lines)

$$F = \frac{|\bar{\phi} - \bar{\phi}_0|}{|\bar{\phi}_0|}, \quad z = -2d, \quad (11)$$

is plotted against the ratio k_t/k_0 for some values of the dielectric loss tangent (assuming that $\varepsilon' = -\varepsilon_0$ and $\mu = -\mu_0$). It can be clearly seen how the transfer function of Eq. (6) is substantially equal to the transfer function for the ideal case, given by Eq. (8), up to a given value of $k_{t,max}$, where it sharply goes to zero. As is shown in the figure, this value of $k_{t,max}$ is given by Eq. (10). Although it is not shown, a similar dependence with magnetic losses was observed.

Thus, the effect of losses on the focusing properties of the slab is a truncation of the inverse of the Fourier integral (4) up to a given value of k_x, k_y given by $k_x^2 + k_y^2 = k_{t,max}^2$. Therefore, a point source will produce a sub-wavelength spot of size $\Delta l \sim 2\pi/k_{t,max}$ at the focus, given by

$$\Delta l \sim \frac{2\pi d}{\ln(2\varepsilon_0/\varepsilon'')}. \quad (12)$$

This condition is consistent with the numerical simulations reported by Ziolkowski et al. [10], which have not shown subwavelength focusing in a LHM slab of thickness $d \sim 3.2\lambda_0(\omega_0)$ and $\varepsilon''/\varepsilon_0 \sim 10^{-3} - 10^{-4}$. However, if thinner LHM slabs and/or smaller losses were considered, the subwavelength focusing would be achieved. The example in Figure 1 of the work of Garcia et al. [8] is also understood in light of Eq. (10), since it corresponds to a case with $|\text{Im}(\beta)|d = 10$ with $\varepsilon''/\varepsilon_0 = 1/5$. The conditions (10) and/or (12) clearly show that, from the standpoint of losses, the real challenge in obtaining perfect lenses is to obtain LHM with very small losses. For usual losses at microwave frequencies ($\varepsilon''/\varepsilon_0 \approx 10^{-4}$) condition (12) shows that the LHM slab thickness must satisfy the condition $d \leq \lambda_0(\omega_0)$.

For paraxial spectral components, that is, for $k_t \ll \omega_0 \sqrt{\mu_0 \varepsilon_0}$, the conditions are $\beta_0 \sim \omega \sqrt{\mu_0 \varepsilon_0}$ and $\beta \sim \omega \sqrt{\mu \varepsilon}$. Thus, the first summand will dominate over the second one in the denominator of Eq. (6) if the slab thickness, d , is smaller than the attenuation length along the LHM, a rather obvious condition. Therefore, Eqs. (6)–(8) also prove the paraxial focusing of monochromatic pointlike sources by LHM slabs.

4. EFFECT OF DISPERSION

Next we will consider the effect of dispersion. For this purpose, we will consider a point source of the kind

$$\mathbf{J} = I_0 \hat{\mathbf{z}} \delta(x) \delta(y) \delta(z) f(t) \exp\{j\omega_0 t\}, \quad (13)$$

where $f(t)$ is a smooth function of time with a maximum at $t = 0$. For the considered source, the scalar potential at the focus plane ($z = -2d$) is given by

$$\phi(x, y, t) = \frac{1}{4\pi^2} \iint \bar{\phi}(k_x, k_y, t) \exp\{-j(k_x x + k_y y)\} dk_x dk_y, \quad (14)$$

with

$$\bar{\phi}(k_x, k_y, t) = \frac{1}{2\pi} \int \bar{\phi}(k_x, k_y, \omega) \tilde{f}(\omega - \omega_0) \exp(j\omega t) d\omega, \quad (15)$$

where

$$\tilde{f}(\xi) = \int f(t) \exp(-j\xi t) dt. \quad (16)$$

We will assume that $f(t)$ is different from zero during a time interval $-\Delta t < t < \Delta t$, so that $f(\omega - \omega_0)$ is meaningful in the interval $\omega_0 - \Delta\omega < \omega < \omega_0 + \Delta\omega$, with $\Delta\omega \sim 2\pi/\Delta t$.

Since the effects of losses have already been considered, we will consider that $\varepsilon(\omega_0) = -\varepsilon_0$ and $\mu(\omega_0) = -\mu_0$. Therefore, losses will be neglected. However, deviations of $\varepsilon = -\varepsilon_0$ and $\mu = -\mu_0$ are expected for $\omega \neq \omega_0$, which can result in limitations to the sub-wavelength focusing similar to those reported in Figure 2. In order to show these limitations with an example, we will consider a medium described by the usual Drude–Lorentz model, given by

$$\mu = \mu_0 \left(1 - \frac{\omega_\mu^2}{\omega_m^2 - \omega^2} \right), \quad (17)$$

$$\varepsilon = \varepsilon_0 \left(1 - \frac{\omega_p^2}{\omega^2} \right), \quad (18)$$

where a plasmlike behavior of the dielectric constant has been supposed in congruence with previous experimental demonstrations [2]. Some specific values for ω_m, ω_μ , and ω_p have been chosen in order to obtain the specific behavior shown in Figure 3. The deviation factor (11) for this specific LHM slab as a function of k_t/k_0 is plotted in Figure 4 for several values of $\Delta f/f_0 = \Delta\omega/\omega_0$. Except for the peaks, which correspond to the excitation of a surface plasmon in the LHM slab, the behavior of F is very similar to that shown in Figure 2. The actual transfer function of Eq. (6) remains almost equal to the ideal transfer function of Eq. (8) until a given $k_{t,max}$, which shows a logarithmic dependence on $\Delta f/f_0$. For the analyzed example and at microwave frequencies ($f_0 \sim 10^9$), pulses of 10 microseconds or more (and very stable sources) are needed to obtain some degree of sub-wavelength focusing. Thus, the limitations to subwavelength focusing imposed by the unavoidable presence of dispersion in LHM slabs are also very strong, a fact which is expressed by the logarithmic dependence with $\Delta f/f_0$, as shown in Figure 4.

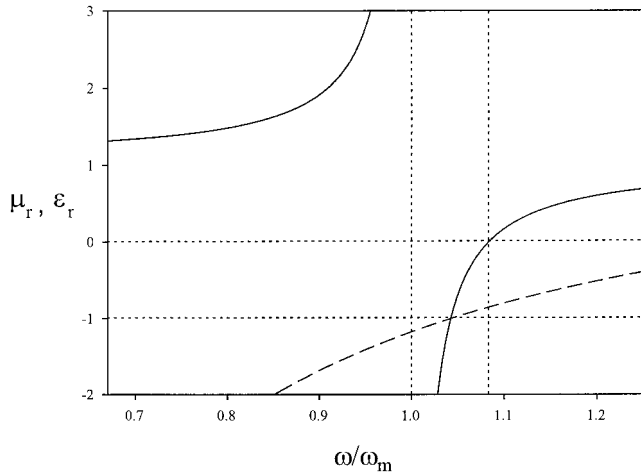


Figure 3 Values of $\mu_r = \mu/\mu_0$ (solid lines) and $\varepsilon_r = \varepsilon/\varepsilon_0$ (dashed line) for the analyzed LHM slab

The finite duration of the RF source also imposes some limitations to the over-wavelength focusing, even if it is assumed that, in its whole frequency band, $\varepsilon \approx -\varepsilon_0$ and $\mu \approx \mu_0$. In that case, the second summand in the denominator of Eq. (6) can be neglected and $\tilde{\phi}(k_x, k_y, \omega)$ is approximated by

$$\tilde{\phi}(z = -2d; \omega) \approx -\frac{I_0}{2\omega\beta_0\varepsilon_0} \exp\{-j(\beta_0 - \beta)d\}. \quad (19)$$

From Eqs. (15) and (19), we obtain

$$\tilde{\phi}(k_x, k_y, t) \approx K \int_{-\Delta\omega}^{\Delta\omega} \tilde{f}(\delta\omega) \exp\{-j(\beta_0 - \beta)d + j(\delta\omega)t\} d(\delta\omega), \quad (20)$$

where $\delta\omega = \omega - \omega_0$ and [see Eq. (8)]

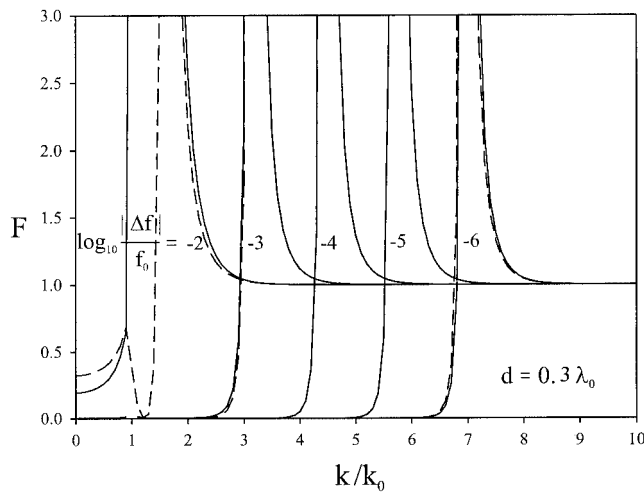


Figure 4 The deviation factor [Eq. (11)] as a function of k/k_0 for an LHM slab with $d = 0.3\lambda_0$ and several values of the relative incremental frequency $\Delta f/f_0$. Positive (negative) values of Δf correspond to solid (dashed) lines

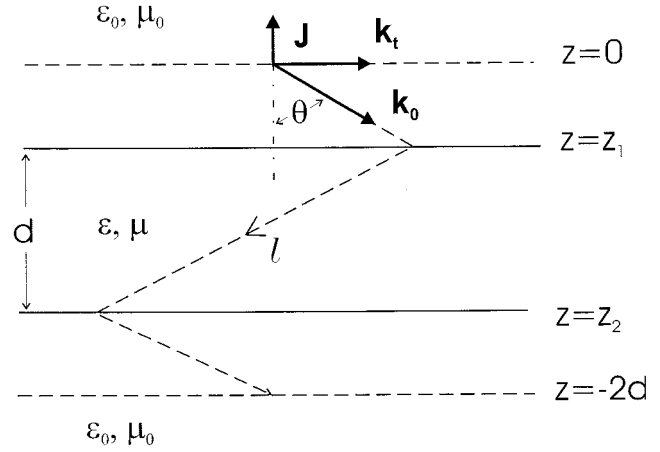


Figure 5 Geometrical interpretation of Eq. (26): when $\varepsilon \approx -\varepsilon_0$ and $\mu \approx -\mu_0$, the source should be switched on for a time that is longer than the travel time of the light between the source and the focus

$$K = -\frac{I_0 \exp(j\omega_0 t)}{4\pi\omega_0\beta_0(\omega_0)\varepsilon_0} = \frac{1}{2\pi} \tilde{\phi}(z=0; \omega_0) \exp\{j\omega_0 t\}. \quad (21)$$

Except for the exponential term, $\exp\{-j(\beta_0 - \beta)d\}$, the integral in Eq. (20) coincides with the expression for $f(t)$ [see Eq. (16)]. Since for $\omega \approx \omega_0$ condition is $\beta \approx \beta_0$, a frequency interval, $\Delta\omega$, can be always found for which

$$\tilde{\phi}(k_x, k_y, t) \approx \tilde{\phi}(z=0; \omega_0) f(t) \exp\{j\omega_0 t\}. \quad (22)$$

In this frequency band, $\Delta\omega$, the corresponding spectral components of the field radiated by the source are almost perfectly reproduced at the focus. The condition for the validity of Eq. (22) can be expressed as

$$|\exp\{-j(\beta_0 - \beta)\} - 1| \ll 1 \quad \text{for} \quad |\omega - \omega_0| < \Delta\omega \sim 2\pi/\Delta t, \quad (23)$$

where Δt is the time interval during which the source is switched on.

Since we are considering over-wavelength spectral-field components, $\exp\{-j(\beta_0 - \beta)d\}$ is a phase factor. After expanding both $\beta(\omega)$ and $\beta_0(\omega)$ in a Taylor series around $\omega = \omega_0$, Eq. (23) can be rewritten as

$$\left| \left(\frac{\partial \beta_0}{\partial \omega} \right)_{\omega_0} - \left(\frac{\partial \beta}{\partial \omega} \right)_{\omega_0} \right| d \Delta\omega \ll 2\pi, \quad (24)$$

or

$$\left| \frac{k_0}{\beta_0(\omega_0)} \right| \left(\frac{1}{c} + \frac{1}{|v_g|} \right) d \Delta\omega \ll 2\pi, \quad (25)$$

where $k_0 = \sqrt{\omega_0^2 \mu_0 \varepsilon_0}$, c is the velocity of light in a vacuum, and v_g is the group velocity in the slab (which is negative in LHM). Note that, for a light ray, the condition is $\beta_0(\omega_0)/k_0 = \cos \theta$ (see Fig. 5). Thus, after some manipulations and taking into account that $\Delta\omega \sim 2\pi/\Delta t$, this last condition is found to be equivalent to

$$\Delta t \gg \frac{l}{c} + \frac{l}{|v_g|}, \quad (26)$$

that is, over-wavelength focusing is achieved if the time interval during which the source is switched on is larger than the travel time of the light between the source and the focus, along the corresponding ray of light. This is a rather intuitive and obvious condition from the standpoint of geometrical optics.

5. CONCLUSION

The focusing properties of physical LHM slabs have been found to be mainly limited by the slab thickness, the material losses, and the dispersive behavior of the LHM, rather than by the free-space wavelength of the incident field. The limitations for sub- and over-wavelength focusing, imposed by material losses and dispersion, have been quantitatively expressed, and numerical examples which illustrate these expressions have been provided. A very strong (logarithmic) dependence of the sub-wavelength focusing properties on both the loss tangent and the dispersive characteristics of the LHM has been found. This strong dependence may constitute a severe limitation from a practical standpoint, but does not constitute a fundamental limit for sub-wavelength focusing. In addition, it has been shown that the condition for over-wavelength focusing of realistic quasimonochromatic sources has a simple and rather intuitive interpretation in terms of geometrical optics.

ACKNOWLEDGMENTS

This work has been supported by the Spanish Ministry of Science and Technology and FEDER funds (project no. TIC2001–3163).

REFERENCES

1. V.G. Veselago, Electrodynamics of substances with simultaneously negative electrical and magnetic properties, *Sov Phys USPEKHI* 10 (1968), 509–517.
2. D.R. Smith, W.J. Padilla, D.C. Vier, S.C. Nemat-Nasser, and S. Schultz, Composite medium with simultaneously negative permeability and permittivity, *Phys Rev Lett* 84 (2000), 4184–4187.
3. R.A. Shelby, D.R. Smith, S.C. Nemat-Nasser, and S. Schultz, Microwave transmission through a two-dimensional, isotropic, left-handed metamaterial, *App Phys Lett* 78 (2001), 489–491.
4. R. Marqués, J. Martel, F. Mesa, and F. Medina, Left-handed media simulation and transmission of EM waves in subwavelength split-ring-resonator-loaded metallic waveguides, *Phys Rev Lett* 89 (2002), 13901(1–4).
5. R. Marqués, J. Martel, F. Mesa, and F. Medina, A new 2D isotropic left-handed metamaterial design: theory and experiment, *Microwave Opt Technol Lett* 36 (2002), 405–408.
6. J.B. Pendry, Negative refraction makes a perfect lens, *Phys Rev Lett* 85 (2000), 3966–3969.
7. R.A. Shelby, D.R. Smith, and S. Schultz, Experimental verification of a negative index of refraction, *Sci* 292 (2001), 77–78.
8. N. García and M. Nieto-Vesperinas, Left-handed materials do not make a perfect lens, *Phys Rev Lett* 88 (2002), 207403(1–4).
9. P.M. Valanju, R.M. Walser, and A.P. Valanju, Wave refraction in negative index media: always positive and very inhomogeneous, *Phys Rev Lett* 88 (2002), 187401(1–4).
10. R. Ziolkowski and E. Heyman, Wave propagation in media having negative permittivity and permeability, *Phys Rev E* 64 (2001), 056625(1–15).
11. R.E. Collin, *Field theory of guided waves*, 2nd ed., IEEE Press, New York, 1991.
12. D.R. Smith, D. Schuring, M. Rosenbluth, S. Schultz, S. Anantha-Ramakrishna, and J.B. Pendry, Limitations on subdiffraction imaging with negative refractive index slab, *App Phys Lett* 82 (2003), 1506–1509.

© 2004 Wiley Periodicals, Inc.

NOISE WAVE MODELING OF MICROWAVE TRANSISTORS BASED ON NEURAL NETWORKS

Vera Marković, Olivera Pronić, and Zlatica Marinković

Faculty of Electronic Engineering
University of Niš
Beogradska 14, 18000 Niš
Serbia and Montenegro

Received 7 November 2003

ABSTRACT: *The noise modeling of microwave FETs based on the noise-wave representation of a transistor-intrinsic circuit is considered. Frequency-dependent noise-wave temperatures are introduced as empirical model parameters and modeled using neural networks. In this way, online optimization in a circuit simulator is shifted to offline training of neural networks. An example of transistor-noise modeling for one specified component is shown.* © 2004 Wiley Periodicals, Inc. *Microwave Opt Technol Lett* 41: 294–297, 2004; Published online in Wiley InterScience (www.interscience.wiley.com). DOI 10.1002/mop.20120

Key words: *microwave transistor; noise modeling; wave approach; neural networks*

1. INTRODUCTION

There are different ways to represent noise in a microwave transistor. A common way is to consider it as composed of a linear noiseless two-port network and two additional noise sources [1]. These noise sources are usually equivalent voltage and/or current sources.

In the last decade, Pospieszalski's approach to noise modeling of MESFETs/HEMTs has gained much attention in microwave community [2]. The noise model he presented is based on an H-shaped representation of transistor intrinsic circuit with two uncorrelated noise sources, one voltage noise source at the gate side and one current noise source at the drain side.

However, at microwave frequencies, a treatment of noise in terms of waves seems more appropriate, allowing the use of scattering matrices for noise computations and leading to advantages in the computer-aided design (CAD) of microwave networks, [3, 4]. In [4], it is shown that the wave approach could be useful for both noise modeling and measurement of microwave FETs. Using a similar approach, new extraction formulas for noise-wave sources in the noise-equivalent circuits of MESFET and HEMT devices, where the correlation between noise sources is included, are derived in [5]. Also, the noise-wave modeling procedure of MEFETs, HEMTs, and dual-gate MESFETs based on a T-shaped representation of a transistor-intrinsic circuit is developed [6]. In that case, three noise-wave temperatures are introduced as empirical noise-model parameters. These temperatures, assumed constant over the whole frequency range, are obtained on the basis of some experimental noise data by applying standard optimization procedures.

In this paper, we propose an improved procedure for MESFET/HEMT noise-wave modeling. Namely, the frequency dependencies of the noise-wave temperatures are included in the transistor-noise model. These frequency dependencies are modeled using neural networks. Neural networks are chosen as a modeling tool, since they have the capability to extract highly nonlinear relationships between two sets of data. Hence, noise temperatures can be computed for any frequency from the desired frequency range, thus yielding a very accurate modeling of noise parameters.